Electron Microscopy Experiments Concerning Hysteresis in the Magnetic Lens System

camera ready version submitted at 08 June 2010 to IEEE Conference on Control Applications (CCA), Multi-Conference on Systems and Control, September 8-10, 2010 Yokohama, Japan

P.J. van Bree, C.M.M. van Lierop, P.P.J. van den Bosch

***Abstract*— Ferromagnetic hysteresis and coupled dynamics in the magnetic lens system of electron microscopes degrade the machine's performance in terms of steady-state error and transition time. To get a clear understanding of the exact problem and the way it is expressed in the application a commercial scanning electron microscope is extended with a data-acquisition and rapid proto-typing system. By means of conditioned experiments the significance of the hysteresis effects for microscopy applications is quantified. The response is evaluated by an analysis of synchronized lens currents and estimated sharpness of the resulting images. The sensitivity of image sharpness versus input variation is obtained in a local operating point. The hysteresis effect and its coupling with dynamics, as a response to changes over the complete working range, result in a significant deviation in image sharpness. Since the magnetic field is not available for measurement, the error is expressed in the quasi-static input variation required to correct for it. In order to get a good understanding of the observed effects and the magnetic lens as a system, an interconnected dynamics-hysteresis-electron optics model is used to analyze and to reproduce the experimental results.**

I. INTRODUCTION

The development of automated applications for electron microscopy is complicated by hysteresis present in the ferromagnetic lenses. The main use of electron microscopes has been high magnification imaging in which a highly trained operator provides the necessary feedback to obtain the optimal settings. Most effort has been in improving the optical resolution from micro-meter down to sub-nanometer scale. During image formation the magnetic field has to be in steady state. This resulted in a design that is highly optimized for *static* use. However, new markets have evolved in which full automation is preferred, [1]. Applications that require a non-periodic change in set-point suffer from steady-state error. An unsharp image in terms of the application. Also the throughput has become a performance indicator which implies that the transition time in between set-points should be as small as possible. The magnetic field distribution within the lens is the quantity that should be controlled. However, magnetic field sensing is complicated by the extreme requirements of electron microscopy in terms of the dynamic range of both frequency and amplitude $(10^5, 10^6)$. Magnetic field sensors are not present in the current microscopes and are, therefore, beyond the scope of this paper. Performance of feedback control based on images (e.g. autofocus by extremum search) is limited by the range in which images have a sufficient signal-to-noise ratio ($< 1\%$ of the input range) and the limited bandwidth (e.g. $70ms/image, \approx 14images/s$). An indication of the required transition time is $< 20ms$ which shows a sampling frequency of $200Hz, 1kHz$ is desired for feedback control. In addition, a large set of specimen does not contain enough information for an autofocus procedure to work.

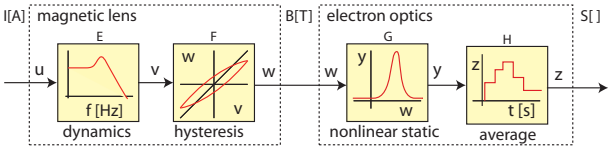

Fig. 1. Interconnected model structure as used to design and analyze the experiments.

The interest in this paper focuses on scanning electron microscopy applications in which large ($> 1\%$ of total range) but non-periodic changes in the magnetic field are required. Examples of large changes required by microscopy applications are the switch in electron acceleration voltage (section II) and ion beam milling, [2]. In the milling application the magnetic field is set close to zero to not influence the milling process and set back to the original value to view the result. The user expects the exact same image sharpness as before the change. Any required corrections limit the throughput. If the input current of the lens is set back to original, since the magnetic field is not available for measurement, the perceived image sharpness will be different as a result of hysteresis in the lens material.

To study the order of magnitude of the errors introduced in open loop, a commercially available scanning electron microscope (FEI Helios [2]) is extended with a dSPACE data-acquisition and rapid prototyping system. Transient current trajectories are applied to the lens system. These trajectories represent a conditioned reconstruction of large changes required in automated applications. All resulting images are recorded. Synchronization of lens input, image sharpness and an animation of the images themselves provides the necessary tool for the control engineer to obtain the control relevant system specifications in agreement with

This work is carried out as part of the Condor project, a project under the supervision of the Embedded Systems Institute (ESI) and with FEI company as the industrial partner. This project is partially supported by the Dutch Ministry of Economic Affairs under the BSIK program.

P.J. van Bree, C.M.M. van Lierop and P.P.J. van den Bosch are with the Department of Electrical Engineering, Eindhoven University of Technology, Postbus 513 5600 MB Eindhoven, The Netherlands p.j.v.bree@tue.nl

the microscopist. Initialization trajectories ensure that despite the hysteresis effect the experiments are made reproducible.

In control engineering, model-based analysis is often used instead or besides actual machine testing. Models have the advantage that the results are easy to reproduce, do not require machine-time and the influence of parameter changes is easy to obtain. Unfortunately, available simulation models (e.g. [3]) taking into account transient inputs for spatial-temporal problems in combination with hysteresis are still in the phase that they only provide approximate solutions to a small set of problems. Currently, it is a major activity in electro magnetics, e.g. [4] in which for instance 3D hysteresis models are under development. The deviation allowed by the highly demanding applications in electron microscopy, is much smaller than the errors provided by the state-of-art models. E.g. [5] provides specifications for the static requirements of lens design. Next to the quantitative error, the qualitative error or behavior of the actual ferromagnetic hysteresis problem for geometries like that of the magnetic lens is not clear. The lack of these models in combination with the lack of a good magnetic field sensor is the main reason to carry out actual machine testing in open loop.

In this paper a phenomenological interconnected series model is introduced in which dynamics, hysteresis and image acquisition are present, Fig 1. This model is used to reconstruct experimental results. The different intermediate signals become available, which makes analysis more understandable. The model can be used as a tool to develop further tests and to illustrate how possible control strategies would work out in perceived sharpness.

II. SCANNING ELECTRON MICROSCOPY

A magnetic electron lens consists of a cylinder shaped coil surrounded by a large (diameter $\approx 25cm$) solid ferromagnetic (e.g. NiFe) pole-piece (yoke). In first instance it can be considered circle symmetric. The magnetic field $B[T]$ observed by the electrons is a function of the geometry and material of the pole-piece and the input current applied to the coil $I[A]$.

In scanning electron microscopy, an electron beam is scanned over the specimen under study (e.g. [6]). The incoming (primary) electrons generate (among other signals) a stream of secondary electrons which are collected by the electron-detector. The number of secondary electrons varies with the material-type and the composition of the sample at the position of the beam.

The trajectory of an electron is influenced by the magnetic field distribution within the lens. The higher the acceleration voltage $\in [0.5, 30kV]$, the higher the speed of the electrons, the higher the absolute value of B must be to project an electron beam with a diameter of $\approx 1\mu m$ into a spot at the surface of the specimen (diameter within $1 - 100nm$). In a simplified view the optimal setting of the lens, resulting in sharp images, is a minimal spot-size. The concept of overfocus and underfocus illustrates that a similar spotsize is possible with two different magnetic field values (Fig. 2).

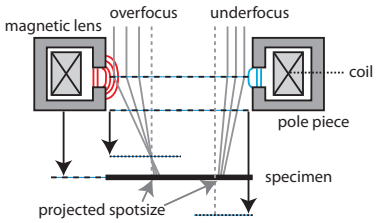

Fig. 2. Schematic representation of the electron trajectory with underfocus (lower magnetic field) and overfocus (higher magnetic field) in a lens. The projected spot-size for the two cases can be equal. The deflection system which is mounted in the lens to enable scanning is not drawn.

III. SHARPNESS

Near the optimal focus, edges appear more intense and the background appears more black than images which are defocused. The pixel intensities p of unsharp images have a smaller deviation from the average intensity (1). This is what variance (2) as a sharpness measure S is based on.

$$\bar{p} = \frac{1}{nm} \sum_{i=1}^{n} \sum_{j=1}^{m} p(i,j), \quad p \in [0,1] \tag{1}$$

$$S = \frac{1}{nm} \sum_{i=1}^{n} \sum_{j=1}^{m} (p(i,j) - \bar{p})^2 \tag{2}$$

S is normalized with respect to the number of pixels ($n \cdot m$), but not for the image content (the composition of the specimen). In the experiments presented in section IV the maximum obtained sharpness is about 0.025. The maximum is a function of the image content and is maximally equal to $S = 0.25$ for an image with $\bar{p} = 0.5$. Zero sharpness would imply a uniform intensity.

In section IV it is illustrated that (2) is not valid for highly unsharp images. However, in this paper the complete analysis is carried out offline and all images are available. Any abnormalities can be checked by studying the corresponding image series. For online implementation of for instance auto-focus, variance may not be the best choice. Other sharpness methods for scanning microscopy applications are topic of current research [7].

IV. EXPERIMENTS

In this section a set of three experiments is presented. First the sensitivity in an operating point $|\Delta S/\Delta I|_I$ is obtained from the I vs. S-graph resulting from quasi-static excitation. Due to slow variation and limited amplitude the influence of hysteresis and dynamic effects are negligible. The second experiment shows hysteresis becomes significant with larger amplitudes. In order to show that the hysteresis effect is coupled with dynamics, the same amplitude trajectories are applied with a different frequency content.

Several side-effects in S are observed. Most of them are related to the fact that it takes time to record a single image and therefore the sharpness measure is not a continuous signal. In order to get a grip on the combination of nonlinear

effects, an phenomenological model of the lens system is introduced in section V.

Since, the magnetic field cannot be measured and the value of S is specimen dependent, the magnitude of the obtained steady state errors are expressed in the amount of input variation required to correct for the error. The total input range of the lens current $I[A] = \pm 2.2A$. Relative input variation is expressed as a percentage of the maximal input variation $(\Delta I/4.4) \cdot 100\%$.

A. Sensitivity

A step-wise quasi-static variation of the lens current in an operating point is applied (Fig. 3). Due to slow variation the influence of dynamics (eddy currents) is negligible. The total variation of the lens current is about 6%. A single period of the excitation in time, illustrates the sharpness $S[]$ variation along with the input profile $I[A]$.

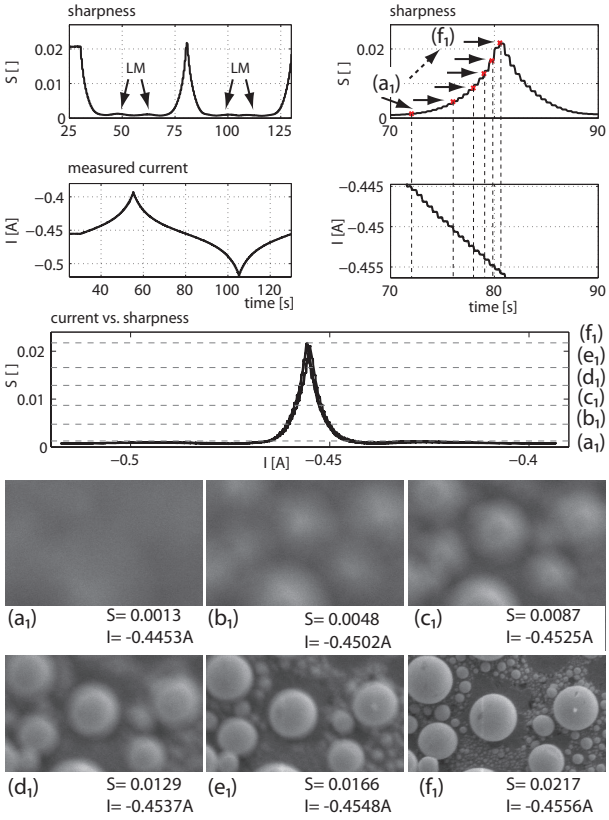

Fig. 3. Sharpness S variation as a response to a quasi-static variation of the input current over $\approx 6\%$. The width of the images as shown represents $\approx 15\mu m$. The distance between lens and specimen is $z \approx 4mm$, electron acceleration voltage, $1kV$. False local maxima in S are indicated with LM.

The I vs. S graph shows the result for two periods of the excitation. An equal projected spot-size in overfocus and underfocus results in a curve that is approximately symmetric with respect to the offset corresponding to optimal focus (Fig. 2). Hysteresis is not significant at this range of input variation. Sensitivity $|\Delta S/\Delta I|$ in terms of images is illustrated by the difference in sharpness of image e_1 and f_1 $((S_{f_1} - S_{e_1})/S_{f_1}) \cdot 100\% = 23\%$ versus the difference in current $\Delta I = 0.02\%$.

The local maxima (LM) observed near zero sharpness (Fig. 3) illustrate the limited validity of this sharpness for highly unsharp images. From construction of the experiments it is clear these maxima are false. Under the condition that the input current is changed very slowly and monotonically increasing (or decreasing) the magnetic field will also be monotonically increasing (or decreasing). The only reason for the sharpness to change in opposite direction is the switch from overfocus to underfocus or vice versa. For the analysis of experiments carried out in this paper it is not of concern; As long as the images are within the sharpness range of between optimal f_1 and the level indicated by image b_1, variance is considered a valid sharpness measure.

B. Initialization

The magnetic lens is open loop stable, in a sense that the magnetic field converges to a constant value for each constant input current. Due to hysteresis, the steady-state output value for a unique constant input value is not unique but can be any value of a set determined by the history of the input. Most demagnetization strategies are based on low-frequency sine waves with decaying envelope of the amplitude. Such sequences are known from magnetic recording [8] and lead to anhysteretic demagnetization. This is an option but not necessary. For this paper, the only requirement after initialization is that a defined constant input I_{dc} results in a magnetic field $B_{dc} \pm \epsilon$. Here ϵ is the allowed error, such that a variation of magnetic field over ϵ still results in similar sharpness. Based on this, the expectation is that a low-frequent sine wave with a large amplitude results in convergence of the magnetic field to a periodic response within a limited number of periods (accommodation to a stable minor loop or limit cycle, [9]). The purpose in this paper is to get into a well defined state for scientific experiments. Here the initialization profile has no strict timing constraints and lasts up to $15s$. For use in automated microscopy, optimization to obtain a minimum initialization time is essential to improve practical value.

Initialization by saturation of the magnetic material is in this case not possible. The geometry and material of the lens (and surrounding vacuum-chamber, etc.) versus the applied magnetic field strength by the lens coil does not result in complete saturation of all involved material. In terms of hysteresis this means that the major loop can not be reached.

The sine-wave initialization profile (2.5 periods of $I = I_{dc} + 0.35\sin(0.5\pi t)$) is applied in two situations with a similar I_{dc} but a different sharpness. Fig. 4 clearly shows the difference between the obtained S values before, and the similarity of the S values after the applied sequence.

A quasi-static stairs excitation with a small amplitude ($A_{stairs} = A_{sin}/159$) is applied before and after the initialization profile in order to check the focal situation (underfocus, overfocus). Only one period is applied, first increasing than decreasing. A lens system in underfocus has a smaller absolute input and, therefore, a lower magnetic field than a system in overfocus.

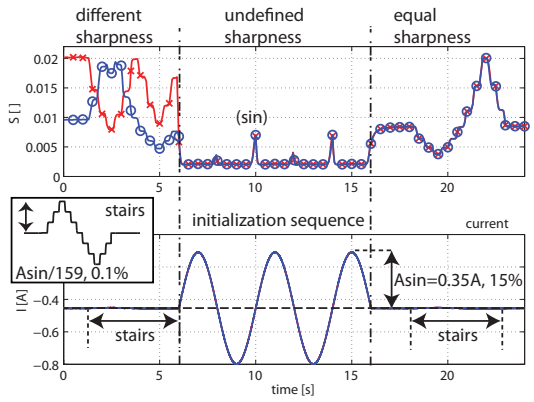

Fig. 4. Initialization profile used: large (15% of total range) but slow sine-wave ($I = I_{dc} + 0.35\sin(0.5\pi t)$). The 2.5 periods of the sine-wave put the magnetic system in the same state (same input I_{dc} and same sharpness S).

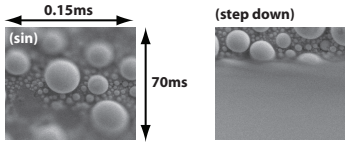

Fig. 5. Examples of images for which the defined sharpness measure is not valid since ΔS is too large during the time a single image is recorded. Image (sin) is recorded during the sine wave excitation indicated in Fig. 4. During the scan of image (step down) a large change in the input is applied (Fig. 7 shows the excitation).

For the example in Fig. 4, the stairs sequence is applied to a negative offset which results in a decrease in absolute input current at the start of the sequence, equal to a decrease in absolute magnetic field. For the line (o) the decreased $|B|$ gains a higher sharpness, meaning that it was slightly overfocused at the start. The line (x) is nearly in optimal focus before the sine is applied, since both an increase and decrease result in decreased sharpness. After the sine-wave the sharpness response of both experiments is similar. The lens system is now in underfocus.

During the initialization profile itself, the sharpness measure is not valid since the assumption that S is constant during the time that an image is recorded is violated. The *(sin)*-image in Fig. 5 shows the effect. The image is sharp in a small region of the image, but blurred in the rest. The scan in horizontal (x) direction takes about $0.15ms$ per line ($300ns$ per pixel, 512 pixels). Scanning a complete frame of 442 lines takes $70ms$ including the time for the electron beam to travel back to the upper left corner.

C. Hysteresis

These experiments provide an estimate of the order of magnitude of the steady state deviation (difference in S) before and after the pulse is applied (Fig. 6). The amplitude of the pulses is different, but the duration is the same ($5s$). The pulses represent a temporary change of operating point of the microscope. For a system without hysteresis the sharpness level after the pulse would converge to the

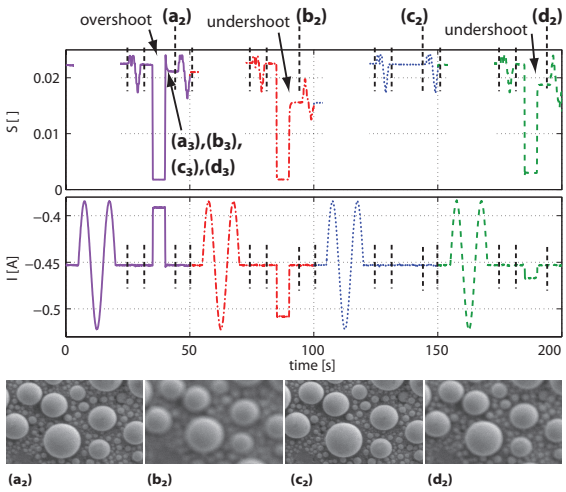

Fig. 6. Sharpness variation as a response to large (10% of total range of $\pm 2.2A$) pulses of different amplitude. The stairs sequences are denoted with the vertical dashed lines.

level from before the pulse, since the same constant input is applied. During each sequence the stairs excitation is applied in between a pulse and initialization in order to compare the order of magnitude of the hysteresis effect to the sharpness variation with a small quasi-static variation. In this way the significance of the effect can be expressed in terms of the input variation required to correct for it.

Image (c_2), Fig. 6 serves as reference since no step is applied. As can be derived from the S-response to the stairs inputs after the pulses (e.g S corresponding to image b_2), the introduced hysteresis effect require a correction in the input larger than the amplitude of the stairs input.

1) Transient effects: The transition-time during the second edge of the pulse is derived from the image sequence. Fig. 7 shows the process of convergence to the steady state. S is already very near its steady state after 3 images ($140ms$). However, S is still changing in between $140ms$ and $1s$ as can be seen from the corresponding plot.

Fig. 6 and 7 show that S can have an overshoot as a response to the pulse. An overshoot in S means that the sharpness is temporarily higher. It is possible that the magnetic field itself has an overshoot. However, it can also be achieved when the optimum of the sharpness function is passed by a monotonically increasing (or decreasing) magnetic field. During both pulses in negative direction (b_2) and (d_2) an undershoot occurs. The phenomena describes can be analyzed in a structured way by using the interconnected series model presented in section V.

D. Hysteresis and Dynamics

In the next experiment the length of the pulses is again $5s$ and the amplitude of all the pulses is the same. However, each pulse is pre-filtered using a 3^{rd}order lowpass filter. It is made sure that no overshoot in the reference signal is introduced by the filter procedure. Four cutoff frequencies are defined: 5, 20, 50 and $100Hz$. The goal is to investigate

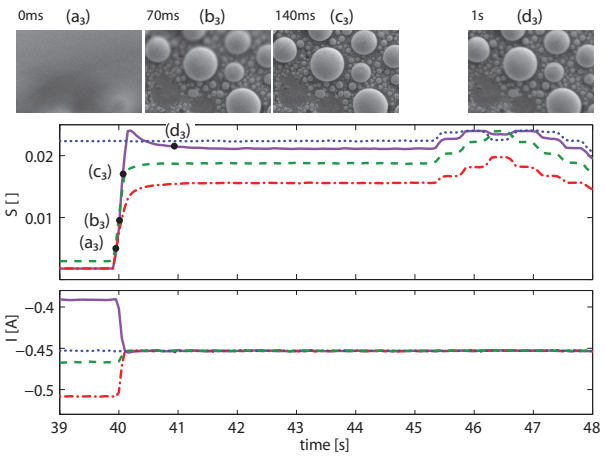

Fig. 7. Convergence of S to constant as a response to the rising edge of a pulse. The images correspond to the pulse shown in Fig. 6, indicated with *overshoot*. The $1^{st}, 2^{nd}, 3^{rd}$ and 15^{th} images after the pulse are shown. The result for all four pulses is shown in a single graph. The current is constant after $50ms$, S requires $\approx 1s$.

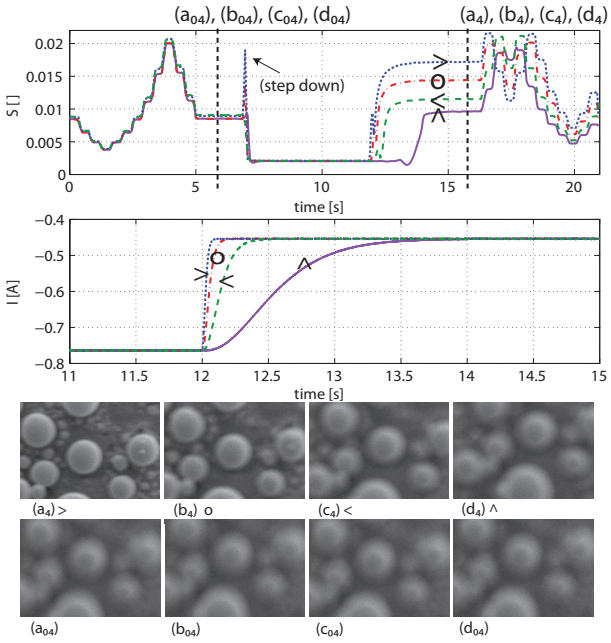

Fig. 8. Sharpness variation as a response to large pulses with 4 pre-filter cutoff frequencies.The current plot is zoomed in on the rising edges to show the difference in excitation. $\wedge 5, < 20, o50$ and $> 100Hz$. The lower row of images corresponds to the start situation at $t = 12.2s$, the upper row the result after the pulse.

whether there is an influence of frequency content on the resulting steady-state value of the magnetic field.

All pulses are preceded by the 2.5 periods of the initializing sine-wave as presented in Fig. 4. Before and after the pulse the stairs excitation is applied. Only the rising edges of the input current are shown, to illustrate the difference of the trajectory in time, Fig. 8.

The response to the stairs excitation before the pulses shows that the initial state is approximately the same. The large peak indicated with *(step down)* is a falsely estimated sharpness value (as illustrated by Fig. 5).

In Fig. 8, the relatively low sharpness of ($\wedge$) compared to ($>$) can be corrected by a change in the input current of about the amplitude of the stairs profile: $2.2mA$. This correction itself is not the objective, but from this it becomes clear that the order of the effect is about 0.05%.

V. INTERCONNECTED MODEL

An interconnected model structure is presented for analysis of the experimental results, Fig 1. An interconnection of a second order linear dynamic system E with a hysteresis model F represents the magnetization dynamics of the magnetic lens. A static positive nonlinear function G describes the relation between magnetic field B and sharpness S. However, this relation is continuous and does not incorporate the *averaging effect* introduced by the image scanning procedure. The filter H, averages the signal y over $70ms$ and corrects for this.

It will be shown that this structure is capable of providing qualitatively the same results as in the experiments. Reconstruction of the (possibly virtual) intermediate signals helps to design the presented test procedure. It is possible to vary the parameters in order to isolate effects, such as sensitivity, hysteresis and coupled hysteresis and dynamics. In that sense the model and the presented experiments were part of an iterative procedure. However, there is no claim that such an block oriented interconnected model is preferred from a behavioral or physical point of view. For instance the intermediate signal v between the dynamic and hysteresis block does not exist in practice and has no physical interpretation.

For the dynamic block E a standard 2^{nd}-order filter is used (3). The hysteresis model F used is a differential equation implementation (4) of a rate-independent semi-linear Duhem model [10], [11]. The parameters of the phenomenological model (three constants) are bounded by $h_3 > 0, h_1 < h_2 < 2h_1$. The positive nonlinear static function, in the model represented by a bell-shaped function (5), represents the BS-curve with similar characteristics to the one observed in Fig. 3.

$$E(s) = \frac{\omega_n^2}{s^2 + 2\zeta\omega_n + \omega_n^2} \tag{3}$$

$$\dot{w} = \dot{v}\left\{\text{sign}(\dot{v})h_3\left[h_2 v - w\right] + h_1\right\} \tag{4}$$

$$G(w) = a_1\left(1 + \left(\frac{w - a_2}{a_3}\right)^2\right)^{-1} \tag{5}$$

A. Simulation

An excitation similar to the dynamics and hysteresis experiments is applied. The input u to the model contains two pulses, pre-filtered (3^{rd}-order) at 20 and $200Hz$. The parameters of the model used in the presented simulation are denoted above the different graphs in Fig. 9. The damping of

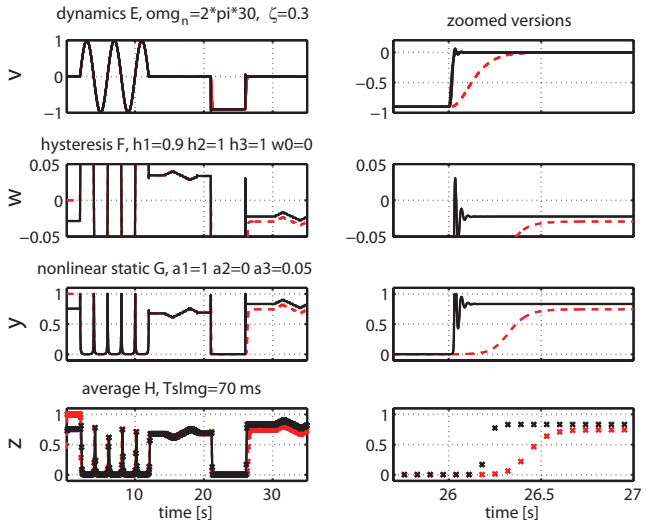

Fig. 9. Simulation of the interconnected model in the time-domain. The difference in the two cases shown is the frequency content of the pulse. One is pre-filtered at $20Hz$ the other at $200Hz$

the second order dynamic block E is low. The low-frequency pulse does not excite the resonance, but the higher frequency one does. This makes that the trajectory of v as input to the hysteresis model is different in a sense that one has overshoot and the other does not. The trajectory in the hysteresis input-output plane is, therefore, different. This difference yields different steady state output values w, which on its turn yields a different sharpness y. The overshoot in the resulting signals w and y is not visible in signal z (Fig. 9) due to the averaging effect introduced by the $70ms$ required to obtain a single image.

VI. CONCLUSIONS AND FUTURE WORKS

A. Conclusions

Hysteresis and dynamics in the ferromagnetic lens system of a scanning electron microscope are the limiting factors in terms of the transition time and steady state error. This paper presents experiments carried out on a commercial state-of-art scanning electron microscope (SEM) extended with a dSPACE data-acquisition and rapid prototyping system. In this way transient non-periodic current trajectories can be designed and tested. The significance of the steady-state errors introduced by hysteresis and coupled dynamics (e.g. eddy currents) is illustrated by the analysis of the estimated sharpness of the resulting images. A synchronized representation of the signals and images presents the problems in a way understandable for both the control engineer and the microscopist.

Three types of experiments are carried out: Quasi-static variation of the lens current provides the sensitivity $|\Delta S/\Delta I|_I$. Due to hysteresis, pulses of different amplitude result in different steady state sharpness levels. However, pulses of equal duration, equal amplitude, but different frequency content also result in different sharpness levels. This proves that there is a coupling between hysteresis and dynamics which should be taken into account to improve the performance of electron microscopy applications. In order to be able to compare the different pulse types, the experiments are made reproducible by means of initialization profiles. Since, the magnetic field is not available as a measured quantity and sharpness highly depends on the operating point, the order of magnitude of the errors is expressed in the amplitude of input variation required to correct for it. An interconnected series model consisting of dynamics, hysteresis, sharpness estimation is introduced to reconstruct the experiment data and to provide intermediate signals.

B. Future Works

In the near future the focus is on the magnetization behavior of the lens itself. A sensor with the required accuracy has recently become available. The experiments presented here are a benchmark for the lens-setup; Similar effects (time-scale, amplitude) should be observed for the magnetic field measurement to be sufficiently accurate to represent the application. The interconnected series model is then used to reconstruct the sharpness signals. The combination of the magnetic lens setup, the actual microscope and models linking both, makes it possible to improve this high accuracy application in a systematic manner.

VII. ACKNOWLEDGMENTS

The authors would like to thank M. Bierhoff (FEI), A.A.S. Sluyterman (FEI), N. Venema (Technolution), W.H.A. Hendrix (TU/e), M. Rudnaya (TU/e) and various others for their help with the microscope setup and processing of the results.

REFERENCES

[1] A. Tejada, S. W. van der Hoeven, A. J. den Dekker, and P. M. J. van den Hof, "Towards automatic control of scanning transmission electron microscopes," *Control Applications, (CCA) & Intelligent Control, (ISIC), 2009 IEEE*, pp. 788–793, 2009.

[2] FEI Company, http://www.fei.com, 2010.

[3] Vector Fields, "Electromagnetic simulation advance helps electrical machinery designers to achieve efficiency," http://www.vectorfields.com/content/view/160/94/, 2009.

[4] E. Dlala, J. Saitz, and A. Arkkio, "Inverted and forward preisach models for numerical analysis of electromagnetic field problems," *IEEE Transactions on Magnetics*, vol. 42, no. 8, pp. 1963–1973, 2006.

[5] B. Lencova, "On magnetic lens computations with fem and bem," *Nuclear Instruments and Methods in Physics Research*, vol. 519, no. 1-2, pp. 133–140, 2004.

[6] L. Reimer, *Scanning electron microscopy: physics of image formation and microanalysis*. Berlin Springer, 1985.

[7] M. Rudnaya, R. M. M. Mattheij, and J. M. L. Maubach, "Iterative autofocus algorithms for scanning electron microscopy," *Microscopy and Microanalysis*, vol. 15, no. SUPPL. 2, pp. 1108–1109, 2009.

[8] E. Della Torre, *Magnetic hysteresis*. IEEE Press, Piscataway, New York, 1999.

[9] P. J. van Bree, C. M. M. van Lierop, and P. P. J. van den Bosch, "Control-oriented hysteresis models for magnetic electron lenses," *Magnetics, IEEE Transactions on*, vol. 45, no. 11, part 2, 2009.

[10] B. D. Coleman and M. L. Hodgdon, “A constitutive relation for rate-independent hysteresis in ferromagnetically soft materials,” *International Journal of Engineering Science*, vol. 24, no. 6, pp. 897–919, 1986.

[11] J. Oh and D. S. Bernstein, “Semilinear duhem model for rate-independent and rate-dependent hysteresis,” *IEEE Trans. Autom. Control*, vol. 50, no. 5, pp. 631–645, 2005.